

The Approach to Stability for Delayed Feedback Control of Chaos for 1-dimensional Maps

J. Keith Thomas and Edward H. Hellen*

University of North Carolina Greensboro,

Department of Physics and Astronomy, Greensboro, NC 27402

(Dated: November 21, 2018)

Abstract

We derive the mathematical form of the approach to stability for a delayed proportional feedback control method applied to a chaotic finite difference 1-dimensional map. Unlike the more common chaos control methods, this method does not use the unstable fixed points or require computational analysis. We verify the mathematical predictions by using an analog electronic circuit realization of a finite difference quadratic return map. Changing the feedback gain produces distinctly different types of approach to stability.

I. INTRODUCTION

It is well known that proportional feedback methods can control chaos for systems described by 1-dimensional maps.^{1,2,3,4} Typically in these methods a system parameter is perturbed by an amount proportional to the difference between the current system value and the unstable fixed point. Pyragas introduced an alternative in which the perturbation is proportional to the difference between the current system value and a previous system value.⁵ This delayed feedback control (DFC) method works without knowledge of unstable fixed points or orbits, and does not require computational analysis. Here we apply this method to finite difference return maps and derive the mathematical form of the approach to stability and verify it experimentally with an electronic circuit. We find a variety of behaviors for the approach to stability depending on the gain of the feedback.

We consider the 1-dimensional finite difference map for system value x with system parameter a

$$x_{n+1} = f(x_n, a_n). \quad (1)$$

Using the DFC method on successive system values, the perturbation of a_n is

$$\Delta a_n = a_n - a_0 = B(x_n - x_{n-1}) \quad (2)$$

where a_0 is the unperturbed parameter value and B is the feedback gain. [So Eq. (1) is equivalent to $x_{n+1} = f(x_n, x_{n-1}, a_0)$]. Feedback is applied only when the magnitude of $(x_n - x_{n-1})$ is within a specified window for control. This method is based on the idea that in a neighborhood of a fixed point of Eq. (1) the difference between successive system values decreases when the distance from the system value to the fixed value decreases. Therefore DFC has the desired property of the perturbation vanishing when the system value attains the unstable fixed value.

We note that the application of DFC to successive system values is essentially a derivative control method since the perturbation uses the difference in system values per iteration.⁶

II. THEORY

The goal here is to predict the behavior of the convergence of system values caused by the control algorithm in Eq. (2). The unperturbed return map is $x_{n+1} = f(x_n, a_0)$. The fixed

point x^* satisfies $x^* = f(x^*, a_0)$. Chaotic behavior is stabilized by perturbing parameter a_n about the value a_0 so as to move the system value x towards the unstable fixed point x^* . A linear expansion of the return map about x^* and a_0 gives

$$x_{n+1} = f(x_n, a_n) = f(x^*, a_0) + f_x(x_n - x^*) + f_a(a_n - a_0) \quad (3)$$

where f_x and f_a are the partial derivatives. This is rewritten as

$$(x_{n+1} - x^*) = f_x(x_n - x^*) + f_a B(x_n - x_{n-1}) \quad (4)$$

where we included our perturbation Eq. (2).

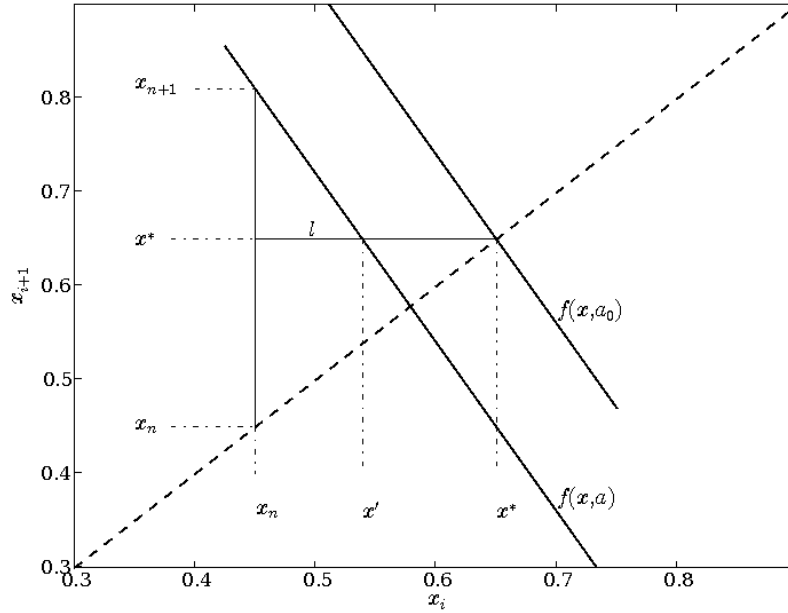


FIG. 1: Portion of return maps showing unperturbed $f(x, a_0)$ and perturbed $f(x, a)$ maps.

Next we remove reference to the fixed point in Eq. (4) expressing it only in terms of differences of successive system values. The derivation is as follows. From the return maps shown in Fig. 1:

$$(x_{n+1} - x_n) = (x_{n+1} - x^*) + (x^* - x_n) \quad (5)$$

and

$$\frac{x_{n+1} - x^*}{l} = -f_x \quad (6)$$

where

$$l = x' - x_n = (x^* - x_n) - \frac{f_a(a - a_0)}{f_x} \quad (7)$$

where we used the result for when x and a are changed while holding $f(x, a)$ constant,

$$\Delta x = -\frac{f_a}{f_x} \Delta a \quad (8)$$

for the case $\Delta x = (x' - x^*)$. Equation (7) becomes

$$(x_n - x^*) = \frac{1}{f_x} (x_{n+1} - x^*) - \frac{f_a}{f_x} B (x_n - x_{n-1}) \quad (9)$$

Using Eq. (9) for the third bracketed term in Eq. (5) and then solving for $(x_{n+1} - x^*)$ gives an expression useful for replacing differences from the fixed point with differences of successive system values.

$$(x_{n+1} - x^*) = \frac{(x_{n+1} - x_n) - \frac{f_a}{f_x} B (x_n - x_{n-1})}{1 - \frac{1}{f_x}} \quad (10)$$

Equation (10) allows us to eliminate the fixed point in Eq. (4) resulting in

$$(x_{n+1} - x_n) = (f_x + f_a B) (x_n - x_{n-1}) - f_a B (x_{n-1} - x_{n-2}) \quad (11)$$

We define $y_n = x_n - x_{n-1}$ and look for solutions $y_n = s^n$. Equation (11) leads to the characteristic equation

$$s^2 - (f_x + f_a B) s + f_a B = 0. \quad (12)$$

Roots are

$$s_{\pm} = \frac{f_x + f_a B}{2} \pm \sqrt{\left(\frac{f_x + f_a B}{2}\right)^2 - f_a B} \quad (13)$$

giving solution

$$y_n = c_1 s_+^n + c_2 s_-^n \quad (14)$$

which converges as long as the larger magnitude root is less than one. So control is achieved (the y_n converge) if

$$f_a B > \frac{-1 - f_x}{2} \quad (15)$$

Limiting case for the smallest magnitude B is thus $B = (1 + f_x) / (-2f_a)$. The sign of B is determined by the sign of f_a . The coefficients c_1 and c_2 are determined by two consecutive values in the sequence $y_0 = c_1 + c_2$ and $y_1 = c_1 s_+ + c_2 s_-$. This gives

$$c_1 = \frac{-s_- y_0 + y_1}{s_+ - s_-} \quad (16a)$$

$$c_2 = \frac{s_+ y_0 - y_1}{s_+ - s_-} \quad (16b)$$

As the magnitude of B is increased the two roots in Eq. (13) merge and are equal when the argument of the square root is zero. This occurs at

$$B = \frac{2\sqrt{1-f_x} - 2 + f_x}{-f_a} \quad (17)$$

and is the transition between smooth (steady) and non-smooth convergence as shown below.

For values of B with larger magnitude the roots are complex conjugates and the convergence is not smooth. The roots are

$$s_{\pm} = \frac{f_x + f_a B}{2} \pm i \sqrt{f_a B - \left(\frac{f_x + f_a B}{2} \right)^2} \quad (18)$$

Using the Euler representation of the complex roots, $s_{\pm} = r e^{\pm i\phi}$, and taking the form of Eq. (14) the solution is

$$y_n = c (r e^{i\phi})^n + c^* (r e^{-i\phi})^n \quad (19)$$

where

$$c = \frac{y_0}{2} + i \left(\frac{y_0 \operatorname{Re}(s_+) - y_1}{2 \operatorname{Im}(s_+)} \right) = c_0 e^{i\theta} \quad (20)$$

Thus the solution is

$$y_n = c_0 e^{i\theta} (r e^{i\phi})^n + c_0 e^{-i\theta} (r e^{-i\phi})^n = 2c_0 r^n \cos(n\phi + \theta) \quad (21)$$

where

$$\phi = \arctan \left(\frac{\sqrt{4f_a B - (f_x + f_a B)^2}}{f_x + f_a B} \right) \quad (22)$$

and

$$\theta = \arctan \left(\frac{y_0 \operatorname{Re}(s_+) - y_1}{y_0 \operatorname{Im}(s_+)} \right) \quad (23)$$

The cosine term causes non-smooth convergence distinctly different from the smooth convergence for the real roots in Eq. (13). Convergence of Eq. (21) occurs when $r < 1$, thus the largest magnitude B that converges is $B = 1/f_a$.

The result is that we predict convergence (control) for feedback gain B between $(1 + f_x)/(-2f_a)$ and $1/f_a$, with Eq. (17) giving the transition from smooth convergence [Eq. (14)] to non-smooth convergence [Eq. (21)].

As an example we consider the 1-dimensional Henon map:

$$f(x, a) = 1 - ax^2 \quad (24)$$

with fixed point

$$x^* = \frac{-1 + \sqrt{1 + 4a_0}}{2a_0} \quad (25)$$

and partial derivatives evaluated at (x^*, a_0)

$$f_x = -2a_0x^* = 1 - \sqrt{1 + 4a_0} \quad (26)$$

$$f_a = -(x^*)^2. \quad (27)$$

For values of a_0 between 1.4 and 2 Eq. (24) displays a variety of unstable behavior including high period oscillations and chaos.⁷ For $a_0 = 1.9$ we find $f_x = -1.93$ and $f_a = -0.259$, so convergence is predicted for values of B between -1.8 and -3.87 with the transition from smooth to non-smooth convergence at -1.96.

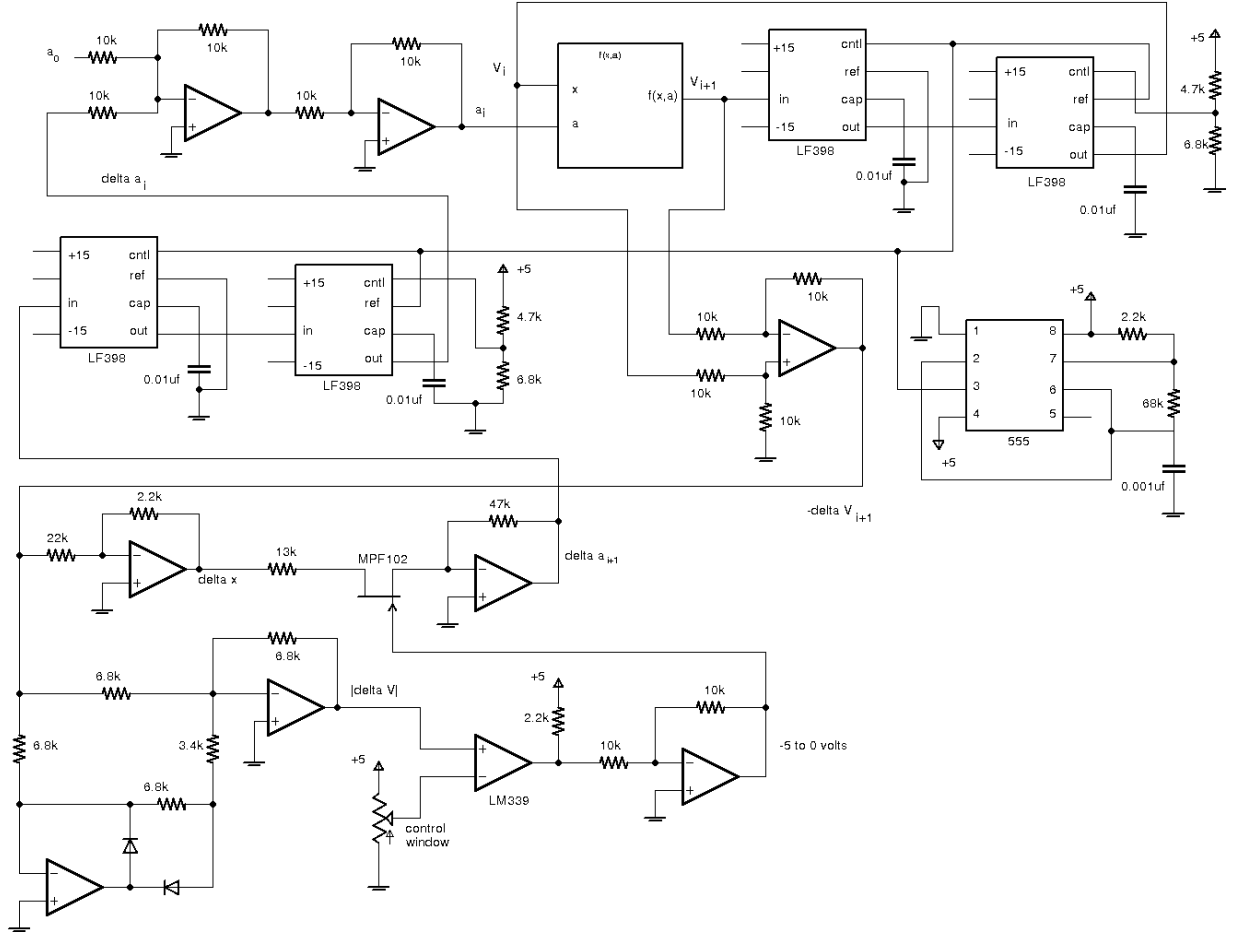


FIG. 2: The circuit for controlling chaotic behavior of the return map $x_{n+1} = f(x_n, a_n)$. Op amps are LF412.

III. CIRCUIT AND MEASUREMENTS

Figure 2 shows the circuitry used to apply the control algorithm to a function block circuit $f(x, a)$ that performs analog computation of a chaotic return map. Here we use the function block circuit shown in Fig 3 that calculates the 1-dimensional Henon map Eq (24).⁷ We have also used function block circuits that produce the Logistic map and the tent map.

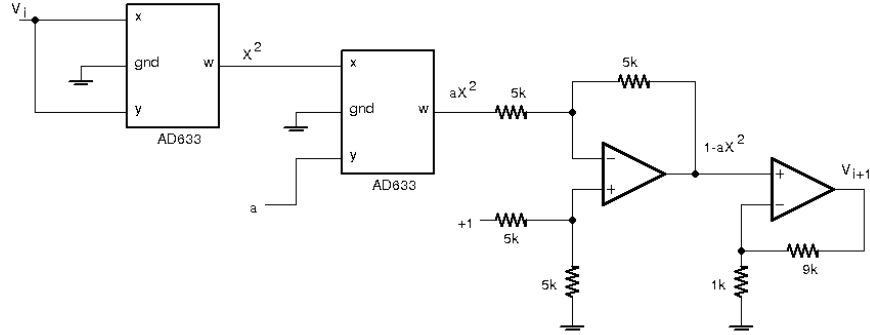


FIG. 3: Henon function block circuit for $f(x, a)$. Relation between voltage and system value is $x = V/10$. The $\times 10$ noninverting amplifier at the output accounts for both a and the $+1$ not being multiplied by 10, the scaling factor of the AD633 multiplier.

At the upper left in Fig 2 the unperturbed parameter value a_0 is added to the perturbation Δa_n to create system parameter a_n . This is input, along with system value voltage V_n , to the $f(x, a)$ circuit block which produces the next system value voltage V_{n+1} . The subtraction op amp creates the difference between the successive system value voltages ΔV_{n+1} that is used to create Δa_{n+1} , the perturbation for the next iteration. ΔV_{n+1} is passed to an absolute value/comparator stage and to a gain stage which produces Δa_{n+1} . The output of the comparison stage (LM339) controls the gate of the FET in the gain stage so that if $|\Delta V|$ is larger than the control window then the gate goes to -5 volts turning off the FET and thereby setting feedback gain $B = 0$. A nonzero value for B is determined by the inverting op amp adjacent to the FET. For the values shown, $47k\Omega$ and $13k\Omega$, $B = -3.6$. The sign of B is easily switched by changing the order of inputs V_n and V_{n+1} to the subtraction amplifier. Prior to the FET $|\Delta V|$ is divided by 10, the scaling factor of the AD633 multiplier used in the $f(x, a)$ circuit block, to convert from voltage $|\Delta V|$ to $|\Delta x|$. The sample/holds (LF398) perform the iteration of n under the control of the 555 timer circuit. With the $68k\Omega$ and $0.001\mu f$ shown in the schematic the period is about $100\mu s$.

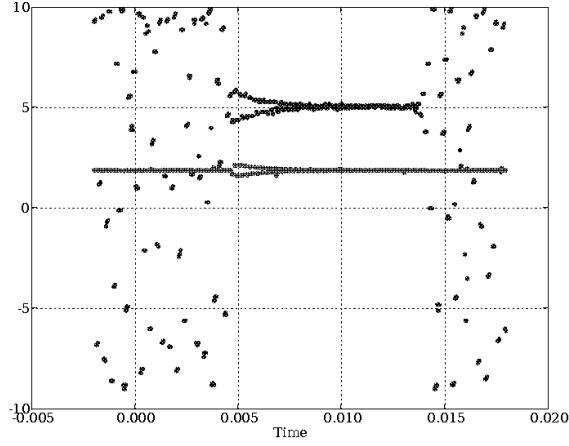


FIG. 4: Data for smooth control of Henon system with feedback gain $B = -1.96$. Control was gated on at $t = 0$ and off at $t = 0.012$. Also shown is the parameter value $a = a_0 + \Delta a$ with $a_0 = 1.9$.

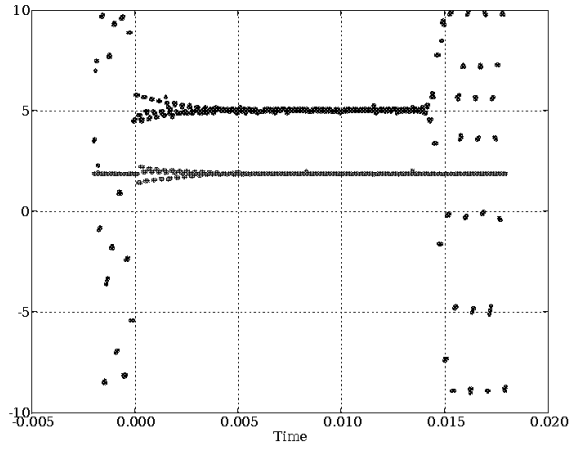


FIG. 5: Data for non-smooth control of Henon system with feedback gain $B = -3.53$. Control was gated on at $t = 0$ and off at $t = 0.012$. Also shown is the parameter value $a = a_0 + \Delta a$ with $a_0 = 1.9$.

Data were collected with a Tektronix TDS 3000 oscilloscope. The control circuit was periodically gated on and off (circuitry not shown) so that it was possible to trigger from the gating signal in order to capture the entire control of chaotic behavior. Figures 4 and 5 show data and the effect of the gating. Also apparent is the control window. Control was

gated on at $t = 0$ in both cases, but in Fig. 4 $|\Delta V|$ was not within the control window until about $t = 4.5$ ms.

IV. RESULTS AND DISCUSSION

Figures 4 and 5 show the effectiveness of the control circuit in Fig 2 when applied to the Henon circuit for $a_0 = 1.9$, a value that gives chaotic behavior. The figures show the measured voltages for the system values $V_n = 10x_n$ and parameter values a_n . Figure 4 uses feedback gain $B = -1.96$ corresponding to the transition between smooth and non-smooth convergence [Eq. (17)], and Fig. 5 uses $B = -3.53$ corresponding to non-smooth convergence.

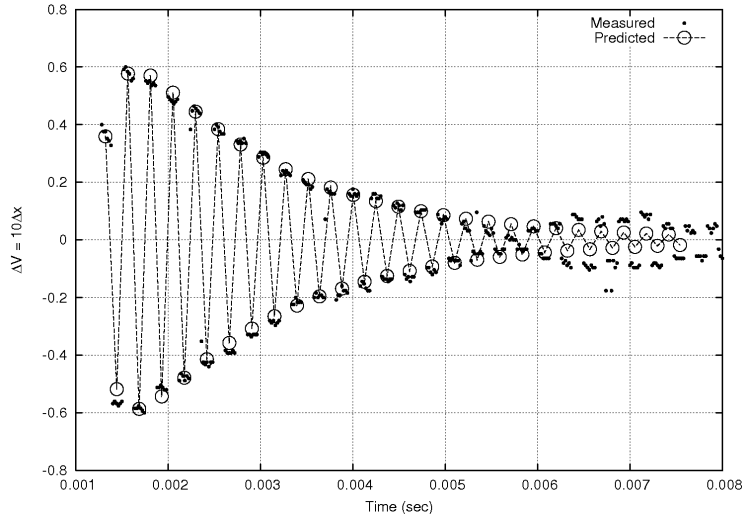


FIG. 6: Data (dots) and prediction (open circles) showing the difference of successive system values $(x_i - x_{i-1})$ for smooth-convergence, $B = -1.9$. The connecting dashed lines are for visual aid only.

The DFC algorithm uses feedback proportional to the difference between successive system values, $y_n = x_n - x_{n-1}$. When the system is successfully controlled $y_n \rightarrow 0$. In Section II we showed that the nature of the convergence of y_n depends on the feedback gain B . The approach to zero for y_n may be smooth [Eq. (14)] or may appear somewhat erratic [Eq. (21)]. Figures 6, 7, and 8 show data and prediction for y_n (actually $\Delta V_n = 10y_n$) for three values of B showing the variety of convergence. Predictions were made by using two successive measured system value differences for y_0 and y_1 in Eqs (16) and (20) to determine

the coefficients for Eqs (14) or (21). The convergence in Fig 6 is smooth and steady, in Fig 7 it appears somewhat erratic, and in Fig 8 a pattern is apparent although the convergence is not steady.

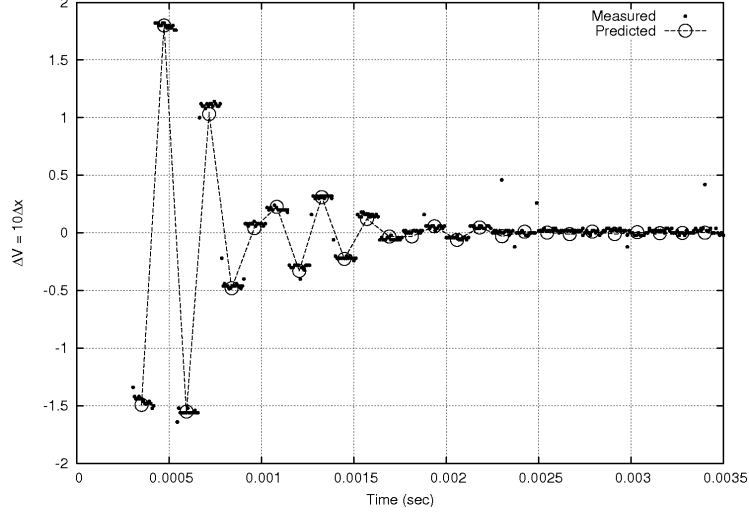


FIG. 7: Data (dots) and prediction (open circles) showing the difference of successive system values $(x_i - x_{i-1})$ for nonsmooth-convergence, $B = -2.3$. Connecting dashed lines are for visual aid only.

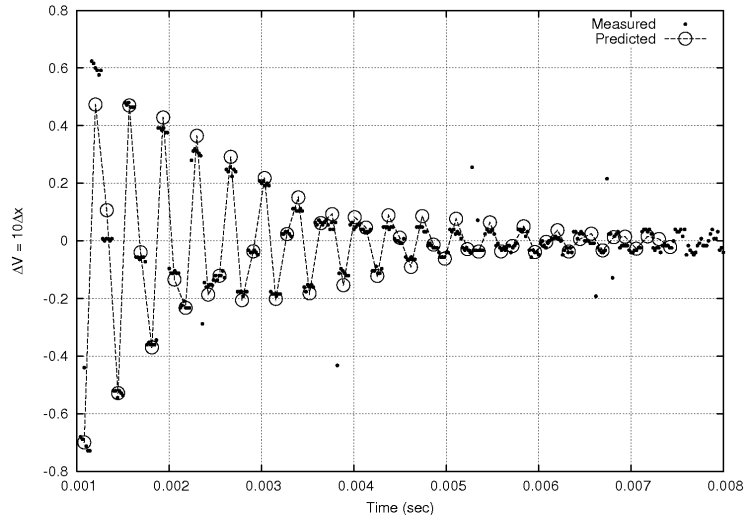


FIG. 8: Data (dots) and prediction (open circles) showing the difference of successive system values $(x_i - x_{i-1})$ for nonsmooth-convergence, $B = -3.5$. Connecting dashed lines are for visual aid only.

For simple proportional feedback using parameter perturbation $\Delta a = K(x_n - x^*)$ applied to the Henon map with $a = 1.9$ the optimal feedback gain is $K = -f_x/f_a = -1.93/0.259 =$

-7.45 .² Half of this value of K is within our predicted range of -1.8 to -3.87 for B using DFC. This is reasonable since by reference to Fig 1 the difference from the system value to the fixed point $(x_n - x^*)$ can be expected to typically be about half of $(x_n - x_{n-1})$, so that the simple proportional feedback method needs gain about twice that of the DFC gain in order to get a similar perturbation Δa .

We have shown that a variety of behavior is expected for the approach to stability when applying DFC to a finite difference 1-dimensional chaotic map. This may be valuable in situations in which the convergence is being closely monitored since erratic and non-steady behavior could be mistaken for a faulty control mechanism. Also, Pyragas pointed out that DFC has advantages in situations where the unstable fixed point is not known or changes with time.

Acknowledgments

This research was supported by an award from the Research Corporation. Corey Clift contributed to early work on this project.

* Electronic address: ehhellen@uncg.edu

- ¹ E. Ott, C. Grebogi, and J. A. Yorke, “Controlling chaos,” *Phys. Rev. Lett.* **64**, 1196-1199 (1990).
- ² R. J. Wiener, K. E. Callan, S. C. Hall, and T. Olsen, “Proportional feedback control of chaos in a simple electronic oscillator,” *Am. J. Phys.* **74**, 200-206 (2006).
- ³ D. J. Gauthier, “Resource Letter: CC-1: Controlling chaos,” *Am. J. Phys.* **71**, 750-759 (2003).
- ⁴ C. Flynn and N. Wilson, “A simple method for controlling chaos,” *Am. J. Phys.* **66**, 730-735 (1998).
- ⁵ K. Pyragas, “Continuous control of chaos by self-controlling feedback,” *Phys. Lett. A* **170**, 421-428 (1992).
- ⁶ P. Parmananda, M. A. Rhode, G. A. Johnson, R. W. Rollins, H. D. Dewald, and A. J. Markworth, “Stabilization of unstable steady states in an electrochemical system using derivative control,” *Phys. Rev. E* **49**, 5007-5011 (1994).
- ⁷ E. H. Hellen, “Real-time finite difference bifurcation diagrams from analog electronic circuits,” *Am. J. Phys.* **72**, 499-502 (2004).